



KfK 3081
September 1980

New Techniques for Multi-Level Cross Section Calculation and Fitting

F. H. Fröhner
Institut für Neutronenphysik und Reaktortechnik
Projekt Schneller Brüter

Kernforschungszentrum Karlsruhe

KERNFORSCHUNGSZENTRUM KARLSRUHE

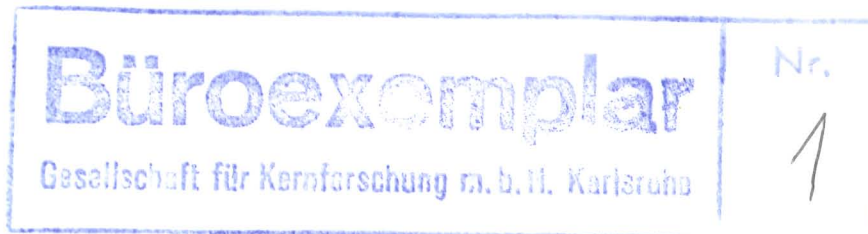
Institut für Neutronenphysik und Reaktortechnik

Projekt Schneller Brüter

KfK 3081

New Techniques for Multi-Level Cross Section
Calculation and Fitting

F. H. Fröhner



Kernforschungszentrum Karlsruhe GmbH, Karlsruhe

Als Manuskript vervielfältigt
Für diesen Bericht behalten wir uns alle Rechte vor

Kernforschungszentrum Karlsruhe GmbH
ISSN 0303-4003

Abstract

A number of recent developments in multi-level cross section work are described. A new iteration scheme for the conversion of Reich-Moore resonance parameters to Kapur-Peierls parameters allows application of Turing's method for Gaussian broadening of meromorphic functions directly to multi-level cross section expressions, without recourse to the Voigt profiles ψ and χ . This makes calculation of Doppler-broadened Reich-Moore and MLBW cross sections practically as fast as SLBW and Adler-Adler cross section calculations involving the Voigt profiles. A convenient distant-level treatment utilizing average resonance parameters is presented. Apart from effectively dealing with edge effects in resonance fitting work it also leads to a simple prescription for the determination of bound levels which reproduce the thermal cross sections correctly. A brief discussion of improved resonance shape fitting techniques is included, with emphasis on the importance of correlated errors and proper use of prior information by application of Bayes' theorem.

Neue Techniken für Berechnung und Anpassung von Vielniveau-Wirkungsquerschnitten

Zusammenfassung

Einige neuentwickelte Methoden für die Arbeit mit Vielniveau-Wirkungsquerschnitten werden beschrieben. Ein neues Iterationsschema für die Umwandlung von Reich-Moore- in Kapur-Peierls-Resonanzparameter ermöglicht Anwendung des Turing-Verfahrens für die Gauß-Verbreiterung meromorpher Funktionen direkt auf Vielniveau-Querschnittsausdrücke, ohne Umweg über die Voigt-Profile ψ und χ . Dies macht die Berechnung von Doppler-verbreiterten Reich-Moore- und MLBW-Querschnitten praktisch ebenso schnell wie SLBW- und Adler-Adler-Querschnittsberechnungen mit den Voigt-Profilen. Eine bequeme Beschreibung der sog. fernen Niveaus mit Hilfe gemittelter Resonanzparameter wird angegeben. Außer wirksamer Beseitigung von Randeffekten bei Resonanzanpassungen liefert sie eine einfache Vorschrift für die Festlegung gebundener Niveaus zur korrekten Wiedergabe der thermischen Querschnitte. Eine kurze Diskussion verbesserter Verfahren zur Formanalyse von Resonanzen ist beigefügt, mit besonderer Berücksichtigung der Bedeutung korrelierter Unsicherheiten und der zweckmäßigsten Verwertung von a-priori-Information mit Hilfe des Satzes von Bayes.

NEW TECHNIQUES FOR MULTI-LEVEL CROSS SECTION
CALCULATION AND FITTING

1. INTRODUCTION

Modern techniques for resonance cross section calculations were reviewed in [1] and in G. Hale's contribution to this conference [2]. Important new developments since the publication of [1] concerning (1) Doppler-broadening of Reich-Moore and multi-level Breit-Wigner (MLBW) cross sections, (2) treatment of distant levels, (3) treatment of bound levels, (4) improvement of conventional least-squares shape analysis by inclusion of correlated errors and prior information via Bayes' theorem are presented in what follows.

This paper was prepared for the Conference on Nuclear Data
Evaluation Methods and Procedures, Brookhaven National Laboratory,
September 22 - 25, 1980

2. WIGNER-EISENBUD AND KAPUR-PEIERLS PARAMETERS

Resonance theory gives the well known relation between the partial cross sections $\sigma_{cc'}$ and the collision matrix (S-matrix) elements $U_{cc'}$ (see [1])

$$\sigma_{cc'} = \pi \lambda_c^2 g_c |\delta_{cc'} - U_{cc'}|^2 \quad (1)$$

where the subscripts c, c' denote entrance and exit channel, respectively, and g_c is the spin factor. The collision matrix is symmetric because the nuclear hamiltonian is invariant under time reversal, and unitary because the probabilities for transitions into the various exit channels must add up to unity. Utilizing the unitarity of U one can express the total cross section σ_c as a linear function of $U_{cc'}$,

$$\sigma_c = \sum_{c'} \sigma_{cc'} = 2\pi \lambda_c^2 g_c (1 - \text{Re } U_{cc}). \quad (2)$$

Therefore the simplest expressions are always obtained for the total cross section whereas the expressions for the elastic-scattering cross section σ_{cc} are always most complicated due to the Kronecker symbol $\delta_{cc'}$ in Eq. (1). It is therefore often more convenient to calculate σ_{cc} as the difference between σ_c and the other partial cross sections than from Eq. (1). Wigner and Eisenbud [3] showed that for nuclear reactions with two collision partners in each channel the collision matrix can be expressed in terms of the resonance parameter matrix R ,

$$U_{cc'} = e^{-i(\phi_c + \phi_{c'})} \left\{ \delta_{cc'} + iP_c^{1/2} \left[(1 - RL^0)^{-1} R \right]_{cc'} P_{c'}^{1/2} \right\}, \quad (3)$$

$$R_{cc'} = \sum_{\lambda} \frac{\gamma_{\lambda c} \gamma_{\lambda c'}}{E_{\lambda} - E}. \quad (4)$$

Alternatively one can write U in terms of the level matrix A [4],

$$U_{cc'} = e^{-i(\phi_c + \phi_{c'})} \left(\delta_{cc'} + i \sum_{\lambda, \mu} \Gamma_{\lambda c}^{1/2} A_{\lambda \mu} \Gamma_{\mu c'}^{1/2} \right), \quad (5)$$

$$(A^{-1})_{\lambda \mu} = (E_{\lambda} - E) \delta_{\lambda \mu} - \sum_c \gamma_{\lambda c} L_c^0 \gamma_{\mu c}, \quad (6)$$

where $L_{cc}^0 = (L_c - B_c) \delta_{cc'} = (S_c - B_c + iP_c) \delta_{cc'}$; $\Gamma_{\lambda c}^{1/2} = \gamma_{\lambda c} \sqrt{2P_c}$. (7)(8)

The boundary parameters B_c are arbitrary. They are prescribed values of the logarithmic derivatives of radial eigenfunctions at the channel radius a_c . For $r_c > a_c$ the nuclear interaction must be negligible, i.e. a_c must be large enough but otherwise it is arbitrary. Both a_c and B_c occur in boundary conditions which, together with the Schrödinger equation, define the radial eigenfunctions for $r_c \leq a_c$ and the eigenvalues E_λ . The width amplitudes $\gamma_{\lambda c}$ are essentially the values of these eigenfunctions at $r_c = a_c$. The E_λ and $\gamma_{\lambda c}$ can be calculated only for simple models such as the shell model or the optical model (cf. e.g. [1]) but normally they are just fit parameters, available for parametrization of the crosssections. The hard-sphere phase shifts ϕ_c and the logarithmic derivatives L_c , on the other hand, can be calculated from the known outgoing wave functions $O_c(r_c)$ for the external region ($r_c \geq a_c$),

$$L_c = a_c \frac{O'_c(a_c)}{O_c(a_c)}, \quad (9)$$

$$\phi_c = \arg O_c(a_c) \equiv \arctan \frac{\text{Im } O_c(a_c)}{\text{Re } O_c(a_c)}. \quad (10)$$

For neutral projectiles the O_c are proportional to the Hankel functions $h_\ell^{(2)}$ of the second kind,

$$O_c(r_c) = ik_c r_c h_\ell^{(2)}(k_c r_c) \\ (\approx i^{-\ell} e^{ik_c r_c} \quad \text{for } k_c r_c \gg \sqrt{\ell(\ell+1)}) , \quad (11)$$

where $k_c = 1/\lambda_c$. The properties of the Hankel functions yield

$$L_o = ik_c a_c = iP_o, \quad L_\ell = -\ell - \frac{(k_c a_c)^2}{L_{\ell-1}^{-\ell}}, \quad (12)$$

$$\phi_o = k_c a_c, \quad \phi_\ell = \phi_{\ell-1} - \arg(L_{\ell-1}^{-\ell}). \quad (13)$$

The energy dependence of L_c^o for photon and fission channels can usually be neglected. The two main versions of the R-matrix formalism differ only by the choice of B_c : The Wigner-Eisenbud version [3] is obtained if B_c is chosen as real and constant. The resonance parameters E_λ , $\gamma_{\lambda c}$ are then also real and constant, and all energy dependences (of R_{cc} , L_c^o , ϕ_c) can be calculated explicitly. The simplest expressions are obtained with the choice $B_c = S_c$ for the photon and fission channels and $B_c = -\ell$ for elastic and inelastic scattering channels. If a_c is taken as small as

possible, i.e. just outside the nuclear interaction sphere, the eigenvalues E_λ coincide essentially with the cross section peaks. The explicitly known energy dependences make the Wigner-Eisenbud version very convenient for most purposes. A certain problem, however, is the required inversion of either a channel matrix, $(1-RL^0)^{-1}$, or a level matrix, A^{-1} , both of which have very high (strictly speaking infinitely high) rank.

The Kapur-Peierls version [5] is obtained if one puts $B_c=L_c$. This eliminates the matrix inversion problem, since $1-RL^0 = 1$, but causes the boundary conditions to be energy dependent so that one has different eigenvalues and -functions for each energy. In other words the eigenfunctions and eigenvalues depend on energy and this energy dependence is specified only indirectly via the boundary conditions. Nevertheless formulae of the Kapur-Peierls type are useful in narrow energy ranges, i.e. for Doppler broadening calculations. We shall write the complex, E-dependent Kapur-Peierls resonance parameters as ϵ_λ , $g_{\lambda c}$ in order to distinguish them from the real, constant Wigner-Eisenbud parameters E_λ , $\gamma_{\lambda c}$. The Kapur-Peierls collision matrix,

$$U_{cc'} = e^{-i(\phi_c + \phi_{c'})} \left(\delta_{cc'} + i \sum_{\lambda} \frac{G_{\lambda c}^{1/2} G_{\lambda c'}^{1/2}}{\epsilon_\lambda - E} \right), \quad (14)$$

contains, in contrast to Eqs. (3) and (5), a simple sum over levels, with complex partial width amplitudes $G_{\lambda c}^{1/2}$ defined by

$$G_{\lambda c} = g_{\lambda c} \sqrt{2P_c} \quad (15)$$

(compare Eq. (8)).

3. THE PRACTICALLY IMPORTANT MULTI-LEVEL APPROXIMATIONS

For parametrization and evaluation of nuclear resonance cross sections three approximations are available,

- the multi-level Breit-Wigner (MLBW) approximation,
- the Adler-Adler approximation,
- the Reich-Moore approximation.

The MLBW approximation is the least, the Reich-Moore approximation the most accurate of these. A convenient starting point for their discussion is the inverse level matrix, Eq. (6), with real and constant (Wigner-Eisenbud) E_λ and $\gamma_{\lambda c}$.

3.1 The Reich-Moore Approximation

Usually many photon channels contribute to the sum in Eq. (6). Their $\gamma_{\lambda c}$ have practically random signs, therefore the off-diago-

nal sums ($\lambda \neq \mu$) tend to be much smaller than the diagonal sums ($\lambda = \mu$). Their omission causes thus only little error. Following Reich and Moore [6] we can therefore write

$$\sum_{c \in \gamma} \gamma_{\lambda c} L_c^0 \gamma_{\mu c} \approx \delta_{\lambda \mu} \sum_{c \in \gamma} \gamma_{\lambda c}^2 L_c^0 \equiv \delta_{\lambda \mu} (-\Delta_{\lambda \gamma} + i\Gamma_{\lambda \gamma}/2). \quad (16)$$

Choosing $B_c = S_c$ for photon channels (\approx const as mentioned before) one gets

$$(A^{-1})_{\lambda \mu} \approx (E_{\lambda} - E - i\Gamma_{\lambda \gamma}/2) \delta_{\lambda \mu} - \sum_{c \notin \gamma} \gamma_{\lambda c} L_c^0 \gamma_{\mu c} \quad (17)$$

This inverse level matrix can be considered as derived from a "reduced" R-matrix with the photon channels eliminated and E_{λ} replaced by $E_{\lambda} - i\Gamma_{\lambda \gamma}/2$,

$$R_{cc'} = \sum_{\lambda} \frac{\gamma_{\lambda c} \gamma_{\lambda c'}}{E_{\lambda} - E - i\Gamma_{\lambda \gamma}/2} \quad (c, c' \notin \gamma). \quad (18)$$

All partial cross sections except that for radiative capture can then be calculated from Eqs. (1) and (3) with the reduced R-matrix instead of the full R-matrix (4). Matrix inversion is no longer a problem for the overwhelming majority of practically important cases: The reduced R-matrix is of rank 1 (an R-function) for all non-fissile nuclei below the lowest inelastic-scattering threshold, and of low rank if few inelastic-scattering or fission channels are open.

This Reich-Moore approximation is exact in the limit of one level or one photon channel (or none) and otherwise it is very accurate. Its non-reduced collision matrix can be considered unitary, and the cross section for radiative capture can either be calculated as the difference

$$\sigma_{c\gamma} = \sigma_c - \sum_{c' \in \gamma} \sigma_{cc'} \quad (19)$$

or from the non-reduced collision matrix with the approximation (16) as

$$\sigma_{c\gamma} = \pi \lambda_c^2 g_c \sum_{\lambda} \Gamma_{\lambda \gamma} \left| \frac{\sum_{c' \notin \gamma} [P^{1/2} (1 - RL^0)^{-1} P^{-1/2}]_{cc'} \Gamma_{\lambda c'}^{1/2}}{E_{\lambda} - E - i\Gamma_{\lambda \gamma}/2} \right|^2 \quad (20)$$

Eq. (20) is the generalization of an expression given for s-wave capture by Harris [7]. The Reich-Moore approximation is very flexible in the sense that a few photon channels, for instance

those with untypically large transition strengths, can be retained and treated explicitly together with the non-photonic channels while the other photon channels are eliminated (cf. [8]). Finally it should be noted that light nuclei are usually treated with phase shift or R-function formulae which can be considered as Reich-Moore formulae for zero radiation width [1].

In spite of these attractive features Reich-Moore parameters were banned from ENDF. One reason may have been the rather obscure description of the Reich-Moore formalism in [9] which makes it look very complicated to the uninitiated. The main reason, however, were the difficulties encountered when Reich-Moore cross sections have to be Doppler broadened. These difficulties no longer exist as explained below.

3.2 The MLBW Approximation

If the off-diagonal elements of the inverse level matrix are neglected altogether (and not just their photon channel components as in the Reich-Moore approximation),

$$\sum_c \gamma_{\lambda c} L_c^O \gamma_{\mu c} \approx \delta_{\lambda\mu} \sum_c \gamma_{\lambda c}^2 L_c^O \equiv \delta_{\lambda\mu} (-\Delta_\lambda + i\Gamma_\lambda/2), \quad (21)$$

inversion of A^{-1} becomes trivial. One obtains the MLBW approximation, with

$$U_{cc'} \approx e^{-i(\phi_c + \phi_{c'})} \left(\delta_{cc'} + i \sum_\lambda \frac{\Gamma_{\lambda c}^{1/2} \Gamma_{\lambda c'}^{1/2}}{E_\lambda + \Delta_\lambda - E - i\Gamma_\lambda/2} \right) \quad (22)$$

This collision matrix is not unitary except in the special case of a single level (single-level Breit-Wigner approximation, SLBW). It therefore tends to yield non-physical cross sections ($\sigma_c > 4\pi\lambda_c^2 g_c$) wherever levels overlap strongly (see Fig. 1). For mild level overlap the MLBW approximation is quite acceptable, however. In any case it is much better than the popular but often very bad approximation, sometimes termed "many-level Breit-Wigner" approximation, which results if cross sections are calculated simply as sums of SLBW terms (plus potential scattering terms in σ_c and σ_{cc}).

In the ENDF format the MLBW approximation is admitted only for elastic scattering. All other partial cross sections are taken as sums over SLBW terms, and the total cross section is the sum of these and the elastic-scattering cross section. Although this prescription ensures that all cross sections are positive it does not prevent wildly unphysical values near the peaks of strongly overlapping resonances. For light and medium-weight nuclei this approximation is therefore often unsatisfactory. Difficulties have also been encountered in the interference minima (windows) of the

total cross sections of structural materials and other light nuclei (Figs. 1a, 1d).

3.3 The Adler-Adler Approximation

The Adler-Adler approximation is obtained if one neglects in Eq. (6) the energy dependence of all L_c^0 , not just that for photon and fission channels. Generalizing the s-wave formulae of Adler and Adler [10] to arbitrary ℓ one can do this in a symmetrical way by taking

$$\sum_c \gamma_{\lambda c} L_c^0(E) \gamma_{\mu c} \approx \sum_c \gamma_{\lambda c} \sqrt{L_c^0(E_\lambda)} \sqrt{L_c^0(E_\mu)} \gamma_{\mu c} . \quad (23)$$

Diagonalization of the inverse level matrix yields then the collision matrix in the form of a pole expansion,

$$U_{cc'} = e^{-i(\phi_c + \phi_{c'})} \left(\delta_{cc'} + i \sum_\lambda \frac{G_{\lambda c}^{1/2} G_{\lambda c'}^{1/2}}{\epsilon_\lambda - E} \right) \quad (24)$$

where $G_{\lambda c} \equiv 2P_c g_{\lambda c}$. In contrast to the Kapur-Peierls parameters of Eqs. (14), (15) the complex Adler-Adler parameters $\epsilon_\lambda, g_{\lambda c}$ do not depend on energy. The approximation (25) means essentially that the energy dependence of level shifts and total widths in the resonance denominators is neglected. Therefore the Adler-Adler approximation works very well for fissile nuclei, where $\Gamma_\lambda \approx \Gamma_{\lambda\gamma} + \Gamma_{\lambda f} \approx \text{const}$, but not so well for light or medium-mass nuclei for which $\Gamma_\lambda \approx \Gamma_{\lambda n} = 2P_\ell(E) \gamma_{\lambda n}^2$ (cf. Fig. 1). Nevertheless it is much better than the MLBW approximation.

A severe test for the accuracy of the various approximations, especially with respect to unitarity, is the calculation of capture cross sections as the difference (19) between total and scattering. For relatively light nuclei this is a small difference between two large numbers so that small violations of unitarity produce very big errors. Calculations for nuclei such as Na or structural materials showed that the Reich-Moore approximation gave results in excellent agreement with Eq. (20) whereas the MLBW and Adler-Adler results were quite useless.

4. DOPPLER BROADENING OF MULTI-LEVEL CROSS SECTIONS

The Kapur-Peierls collision matrix (14) yields cross section expressions which can be written in the concise form

$$\sigma_c = 4\pi\lambda_c^2 g_c \left\{ \sin^2 \phi_c + \text{Re} \left[e^{-2i\phi_c} \sum_\lambda \frac{G_{\lambda c}}{G_\lambda} (\psi_\lambda + i\chi_\lambda) \right] \right\} , \quad (25)$$

$$\sigma_{cc'} = \sigma_c \delta_{cc'} - 4\pi\lambda^2 g_c \operatorname{Re} \left[\sum_{\lambda} \frac{G_{\lambda c}^{1/2} G_{\lambda c'}^{1/2}}{G_{\lambda}} W_{cc'}(\mathbf{E}_{\lambda}^*)^* (\psi_{\lambda} + i\chi_{\lambda}) \right], \quad (26)$$

$$\text{where } W_{cc'}(\mathbf{E}_{\lambda}^*) = \delta_{cc'} + i \sum_{\mu} \frac{G_{\mu c}^{1/2} G_{\mu c'}^{1/2}}{\mathbf{E}_{\mu} - \mathbf{E}_{\lambda}^*}, \quad (27)$$

$$\psi_{\lambda} + i\chi_{\lambda} = \frac{iG_{\lambda}/2}{\mathbf{E} - \mathbf{E}_{\lambda}} = \frac{G_{\lambda}^2/4}{(\mathbf{E} - \mathbf{E}_{\lambda}')^2 + G_{\lambda}^2/4} + \frac{i(\mathbf{E} - \mathbf{E}_{\lambda}')G_{\lambda}/2}{(\mathbf{E} - \mathbf{E}_{\lambda}')^2 + G_{\lambda}^2/4}, \quad (28)$$

$$\text{with } G_{\lambda} \equiv -2\operatorname{Im}\mathbf{E}_{\lambda}, \quad \mathbf{E}_{\lambda}' \equiv \operatorname{Re}\mathbf{E}_{\lambda}. \quad (29)$$

The functions ψ_{λ} , χ_{λ} are the symmetric and asymmetric Breit-Wigner line shapes. They contain the main (resonance-type) energy dependence, all other quantities vary slowly with energy. Therefore Doppler broadening with the usual Gaussian kernel requires simply that ψ_{λ} and χ_{λ} be taken as the Voigt profiles

$$\psi_{\lambda} = \frac{1}{\Delta\sqrt{\pi}} \int_{-\infty}^{\infty} d\mathbf{E}' e^{-(\mathbf{E}' - \mathbf{E})^2/\Delta^2} \frac{G_{\lambda}^2/4}{(\mathbf{E}' - \mathbf{E}_{\lambda}')^2 + G_{\lambda}^2/4}, \quad (30)$$

$$\chi_{\lambda} = \frac{1}{\Delta\sqrt{\pi}} \int_{-\infty}^{\infty} d\mathbf{E}' e^{-(\mathbf{E}' - \mathbf{E})^2/\Delta^2} \frac{(\mathbf{E}' - \mathbf{E}_{\lambda}')G_{\lambda}/2}{(\mathbf{E}' - \mathbf{E}_{\lambda}')^2 + G_{\lambda}^2/4}, \quad (31)$$

where $\Delta = \sqrt{4EkT/A}$ is the Doppler-width (kT : Lamb-corrected temperature in energy units, A : target/projectile mass ratio), cf. [1]. If we consider neutron cross sections for specific reactions (total, (n,n) , (n,f) , (n,γ) , ...) rather than for specific channels (c, c') we can write, in the notation of Adler and Adler [10],

$$\sigma_t \equiv \sum_{c \in n} \sigma_c = \sigma_p + \frac{1}{\sqrt{E}} \sum_{\lambda} \frac{1}{v_{\lambda}} \left(G_{\lambda}^{(t)} \psi_{\lambda} - H_{\lambda}^{(t)} \chi_{\lambda} \right), \quad (32)$$

$$\sigma_x \equiv \sum_{c \in n} \sum_{c' \in x} \sigma_{cc'} = \frac{1}{\sqrt{E}} \sum_{\lambda} \frac{1}{v_{\lambda}} \left(G_{\lambda}^{(x)} \psi_{\lambda} - H_{\lambda}^{(x)} \chi_{\lambda} \right), \quad (x=n, \gamma, f) \quad (33)$$

where σ_p is the potential-scattering cross section, $G_{\lambda}^{(x)}/(\sqrt{E}v_{\lambda})$ and $H_{\lambda}^{(x)}/(\sqrt{E}v_{\lambda})$ are sums over all coefficients of ψ_{λ} and χ_{λ} in Eqs. (25) and (26), with $v_{\lambda} \equiv G_{\lambda}/2$ and \sqrt{E} coming from $\lambda^2 P_c$. The

level sums run over all contributing levels irrespective of $J\pi$, the spin factors g_c being absorbed in the Adler-Adler coefficients $G_\lambda^{(x)}$, $H_\lambda^{(x)}$.

Eqs. (32), (33) show that Doppler-broadened multi-level cross sections can be calculated most conveniently with the Voigt profiles if the Adler-Adler parameters $\epsilon_\lambda = \mu_\lambda + i\nu_\lambda$, $G_\lambda^{(x)}$, $H_\lambda^{(x)}$ are available. In MLBW approximation one must use Eqs. (25) and (26), with $G_{\lambda c} = \Gamma_{\lambda c}$, $G_\lambda = \Gamma_\lambda$ (compare Eqs. (14) and (22)). This, however, is time-consuming if many levels are to be included, because double sums over levels must be calculated for $\sigma_{cc'}$ (over λ in Eq. (26), over μ in Eq. (27)). The Voigt profiles cannot be used directly with the Reich-Moore approximation. Of course, it is always possible to convert a set of Reich-Moore parameters to Kapur-Peierls parameters at a given energy. For $\ell = 0$ this can be done e.g. with the POLLA code [11]. More generally Wigner-Eisenbud parameters can be converted to Kapur-Peierls parameters as follows [12]. The collision matrix must be invariant under the corresponding change of boundary parameters (e.g. from $B_c = -\ell$ to $B'_c = L_c$). This means $(1-RL^0)^{-1}R = R'$, if R' denotes the Kapur-Peierls R -matrix corresponding to B'_c . With the abbreviations

$$K \equiv L^{01/2} R L^{01/2}, \quad K' = L^{01/2} R' L^{01/2} \quad (34)$$

one has

$$(1-K)^{-1} = 1+K' \quad (35)$$

The Kapur-Peierls resonance energies are the complex poles ϵ_λ of R' and K' , i.e. the solutions of

$$\det[1-K(\epsilon_\lambda)] = 0 \quad (36)$$

The residues of R' at the pole ϵ_λ are

$$g_{\lambda c} g_{\lambda c'} = \frac{1}{\sqrt{L_c^0 L_{c'}^0}} \frac{\text{cof}[1-K(\epsilon_\lambda)]_{cc'}}{\sum_{c,c'} \dot{K}(\epsilon_\lambda)_{cc'} \text{cof}[1-K(\epsilon_\lambda)]_{cc'}} \quad (37)$$

where cof denotes the cofactor matrix ($\text{cof}X = X^{-1} \det X$ for non-singular X), and

$$\dot{K}(E)_{cc'} \equiv \left[L^{01/2} \frac{\partial R}{\partial E} L^{01/2} \right]_{cc'} = \sqrt{L_c^0 L_{c'}^0} \sum_{\lambda} \frac{\gamma_{\lambda c} \gamma_{\lambda c'}}{(E_\lambda - E)^2} \quad (38)$$

Eqs. (37), (38) follow from Eq. (35) in the limit $E \rightarrow \epsilon_\lambda$, where L^0 is considered as unaffected by the limiting process. Eq. (36)

can be solved by iteration. Denoting the trace of a matrix by tr we write

$$\det(1-K) = 1 - \text{tr}K + F, \quad (39)$$

where $-\text{tr}K + F$ is the sum of $\det(-K)$ and all principal minors of $\det(-K)$ (see e.g. [13]),

$$\begin{aligned} F &= 0 && \text{for 1 (elastic) channel} \\ F &= \det(-K) && \text{for 2 channels} \\ F &= \det(-K) + \text{tr cof}(-K) && \text{for 3 channels} \\ &\text{etc.} \end{aligned}$$

Next we write, in Wigner-Eisenbud representation,

$$-\text{tr}K(\mathbf{E}_\lambda) = - \sum_{\mu} \frac{1}{E_{\mu} - \mathbf{E}_\lambda} \sum_c L_c^o \gamma_{\mu c}^2 = \sum_{\mu \neq \lambda} \frac{\Delta_{\mu} - i\Gamma_{\mu}/2}{E_{\mu} - \mathbf{E}_\lambda} + \frac{\Delta_{\lambda} - i\Gamma_{\lambda}/2}{E_{\lambda} - \mathbf{E}_\lambda}, \quad (40)$$

where the definition (21) is used. Insertion of (39) with (40) in (36) yields

$$\mathbf{E}_\lambda = E_\lambda + \frac{\Delta_{\lambda} - i\Gamma_{\lambda}/2}{1 + \sum_{\mu \neq \lambda} \frac{\Delta_{\mu} - i\Gamma_{\mu}/2}{E_{\mu} - \mathbf{E}_\lambda} + F(\mathbf{E}_\lambda)}. \quad (41)$$

This equation is readily solved by iteration, starting with the rather plausible initial approximation $\mathbf{E}_\lambda \approx E_\lambda + \Delta_{\lambda} - i\Gamma_{\lambda}/2$. In Reich-Moore approximation E_{μ} must be replaced by $E_{\mu} - i\Gamma_{\mu\gamma}/2$, Γ_{μ} by $\Gamma_{\mu} - \Gamma_{\mu\gamma}$ everywhere. Once \mathbf{E}_λ is known with sufficient accuracy one can calculate the residues with Eq. (37). Fig. 2 shows natural cross sections calculated from Reich-Moore parameters directly and from the Kapur-Peierls cross section expressions (25) - (29) after conversion of the Reich-Moore parameters according to Eqs. 37 - 41. The relative differences were of order 10^{-4} for σ_{γ} and of order 10^{-5} for all other cross sections. One can use this prescription to establish, at each energy of a suitably chosen grid, the Kapur-Peierls parameters and then calculate Doppler-broadened cross sections with the Kapur-Peierls expressions (25) - (29) involving the Voigt profiles. This requires the same time as is needed for a similar MLBW calculation plus the time needed for parameter conversion at each energy. Test calculations showed that about three times as much computer time is needed for Reich-Moore cross sections as for MLBW cross sections [12]. Fortunately one can reduce the time requirements for both Reich-Moore and MLBW cross sections drastically (in fact to about those for SLBW calculation) if one does not insist on using the Voigt profiles. It turns out that a method available for fast calculations of ψ and χ can be applied directly to multi-level cross sections.

5. TURING'S METHOD FOR GAUSSIAN BROADENING
OF MEROMORPHIC FUNCTIONS

Bhat and Lee-Whiting [14] showed that the Voigt profiles can be calculated very fast with a method developed by Turing for Gaussian broadening of meromorphic functions (functions with given poles). It so happens that the combination $\psi + i\chi$ represents the simplest case of such a function, one single pole:

$$\begin{aligned} \psi + i\chi &= \frac{1}{\Delta\sqrt{\pi}} \int_{-\infty}^{\infty} dE' e^{-(E'-E)^2/\Delta^2} \frac{i\Gamma/2}{E'-E_0 + i\Gamma/2} \\ &= \frac{iy_0}{\sqrt{\pi}} \int_{-\infty}^{\infty} dx \frac{e^{-x^2}}{x-z_0} \end{aligned} \quad (42)$$

$$\text{with } x \equiv \frac{E'-E}{\Delta}, \quad z_0 = x_0 + iy_0 \equiv -\frac{E-E_0 + i\Gamma/2}{\Delta} \quad (43)$$

To calculate the integral in (42) Turing [15] considered the contour integral (see Fig. 3)

$$\begin{aligned} \int_C dz \frac{e^{-z^2}}{z-z_0} \frac{1}{1-e^{2\pi iz/h}} &= 2\pi i \left(\sum_{n=-\infty}^{\infty} \frac{e^{-n^2 h^2}}{nh-z_0} \frac{h}{-2\pi i} + \frac{e^{-z_0^2}}{1-e^{2\pi iz_0/h}} P \right) \\ &= \int_{\infty+i\pi/h}^{-\infty+i\pi/h} dz \frac{e^{-z^2}}{z-z_0} + \int_{\infty+i\pi/h}^{-\infty+i\pi/h} dz \frac{e^{-z^2}}{z-z_0} \frac{e^{2\pi iz/h}}{1-e^{2\pi iz/h}} \\ &\quad + \int_{-\infty-i\pi/h}^{\infty-i\pi/h} dz \frac{e^{-z^2}}{z-z_0} \frac{1}{1-e^{2\pi iz/h}} \end{aligned} \quad (44)$$

where $P = \begin{Bmatrix} 0 \\ 1/2 \\ 1 \end{Bmatrix}$ for $y_0 \begin{Bmatrix} > \\ = \\ < \end{Bmatrix} \pi/h$.

For $y_0 < 0$ the path of integration for the first integral in the last line can be shifted to the real axis. Furthermore, an upper limit can be established for the absolute square of the last two integrals (cf. [14]). The result is

$$\begin{aligned} \psi+i\chi = & \frac{1}{\Delta\sqrt{\pi}} \sum_{n=-\infty}^{\infty} \delta E e^{-(E_n-E)^2/\Delta^2} \frac{i\Gamma/2}{E_n-E_0+i\Gamma/2} + \\ & + \sqrt{\pi} \frac{\Gamma}{\Delta} \frac{e^{-(E-E_0+i\Gamma/2)^2/\Delta^2}}{1-e^{-2\pi i(E-E_0+i\Gamma/2)/\delta E}} P + F \end{aligned} \quad (45)$$

$$\text{where } \delta E = h \cdot \Delta, \quad E_n = E+n\delta E, \quad (46)$$

$$P = \left\{ \begin{array}{c} 0 \\ 1/2 \\ 1 \end{array} \right\} \text{ for } \frac{\Gamma/2}{\Delta} \left\{ \begin{array}{c} > \\ = \\ < \end{array} \right\} \pi \frac{\Delta}{\delta E}, \quad (47)$$

$$|F| \leq \frac{2}{\sqrt{\pi}} \left[1 + \left(\frac{E-E_0}{\Gamma/2} \right)^2 \right]^{1/2} \left| 1 - \left(\frac{2\pi\Delta}{\Gamma\delta E} \right)^2 \right|^{-1} \frac{e^{-(\pi\Delta/\delta E)^2}}{1-e^{-2(\pi\Delta/\delta E)^2}} \quad (48)$$

The factor $\exp[-(\pi\Delta/\delta E)^2]$ is extremely small for $\delta E < \Delta$. Neglecting F, Bhat and Lee-Whiting obtained accuracies of 10^{-7} or better for ψ and χ with $\delta E/\Delta \approx 0.7$. Eq. (45) shows then that Turing's approximation is essentially a simple sum approximation to the integral (sum term) plus a correction term which appears only if the pole is narrow compared to the grid of the sum term ($P > 0$ only if $\Gamma/2 \leq \pi\Delta^2/\delta E$). The grid in turn is to be taken as somewhat smaller than the Doppler width. Moreover, even for relatively narrow poles the pole term can be neglected if the pole is not close to E because of its proportionality to $\exp[-(E-E_0)^2]$. For essentially the same reason one needs only sum terms with $-5 \lesssim n \lesssim 5$. Many group constant and resonance analysis codes calculate the Voigt profiles with this fast technique.

If one applies Turing's method to each term in the Kapur-Peierls cross section expressions (25), (26) one gets again a sum approximation to the integral plus correction terms for narrow, nearby poles, e.g.

$$\begin{aligned} \sqrt{E} \bar{\sigma}_c(E) \approx & \frac{1}{\Delta\sqrt{\pi}} \sum_{n=-N}^N \delta E e^{-(E_n-E)^2/\Delta^2} \sqrt{E_n} \sigma_c(E_n) \\ & + \pi\sqrt{E} \sum_{\lambda} C_{\lambda} G_{\lambda} \frac{e^{-(E-E_{\lambda})^2/\Delta^2}}{1-e^{-2\pi i(E-E_{\lambda})/\delta E}} P_{\lambda} \end{aligned} \quad (49)$$

where C_{λ} is the coefficient of $\psi_{\lambda}+i\chi_{\lambda}$ in Eq. 25. Now the unbroadened cross section $\sigma_c(E_n)$ can be calculated directly with Eqs. 2, 3 and 18 from the unconverted Reich-Moore parameters. Since no double sums are needed this calculation is about as fast as an

SLBW calculation. The pole term, on the other hand, requires the Kapur-Peierls parameters \mathcal{E}_λ , G_λ , but because of the factor P_λ (cf. Eq. (47)) only for relatively narrow resonances, and only near their peaks. In these narrow energy ranges one can neglect the energy dependence of C_λ , G_λ and \mathcal{E}_λ . It is therefore sufficient to convert parameters and to calculate the coefficients C_λ at only very few energies, namely at the formal resonance energies of the narrow resonances, $E'_\lambda = \text{Re } \mathcal{E}_\lambda$ (Eq. (29)). The time for calculation of the sum terms and pole terms is essentially the same as in SLBW calculations. The only additional time required is that for conversion to Kapur-Peierls parameters at few energies. For large numbers of levels this is only a small fraction of the total time. The Doppler width appearing as the natural mesh size in Turing's method makes it very convenient for resonance shape fitting.

The same technique can be used for MLBW cross sections. In this case the Kapur-Peierls parameters are simply $\mathcal{E}_\lambda = E_\lambda + \Delta\lambda - i\Gamma_\lambda/2$, $g_{\lambda c} = \gamma_{\lambda c}$, and no conversion is needed at all. Thus the calculation is practically as fast as an SLBW calculation, the time required increasing linearly with the number of levels, whereas the time required for a $\sigma_{cc'}$ calculation with the Voigt profiles increases quadratically with the number of levels because of the double sum in Eq. (26).

The Gaussian broadening in Eqs. (30) and (31) is not quite exact. For the free-gas model the exact kernel was given by Solbrig [16]. Formally it is identical to the Watt spectrum used to describe fission neutron spectra [17], i.e. to a Galileo-transformed Maxwellian spectrum. In terms of speeds one can write

$$v^2 \bar{\sigma}_{cc'}(v) = \frac{1}{v_T \sqrt{\pi}} \left[\int_{-\infty}^{\infty} dv' e^{-(v'-v)^2/v_T^2} v'^2 \sigma_{cc'}(v') - 2 \int_0^{\infty} dv' e^{-(v'+v)^2/v_T^2} v'^2 \sigma_{cc'}(v') \right] \quad (50)$$

where $E = mv^2/2$, $kT = Mv_T^2/2$ (m : neutron mass, M : target-nuclear mass). The second integral is negligible for $E \gtrsim 4kT/A$, so that above a few meV this is again a Gaussian convolution of $|\delta_{cc'} - U_{cc'}|^2$ for $\sigma_{cc'}$ (and of $1 - \text{Re}U_{cc}$ for σ_c) which can be calculated with Turing's method, the poles being located at $v_\lambda = \pm \sqrt{2\mathcal{E}_\lambda/m}$. This approach is implemented in the newly developed Doppler-broadening code DOBRO. Fig. 4 shows an example where a 3-channel Reich-Moore calculation, with 35 levels included explicitly, yielded a complete set of cross sections in 3.7 seconds.

6. LEVEL-STATISTICAL TREATMENT OF DISTANT LEVELS

Modern evaluated files contain parameters for hundreds of levels. Such large numbers suggest a level-statistical treatment of the more distant levels as an additional means to speed up the calculations. The easiest and most direct way to do this is to split the R-matrix into a local and a distant-level term,

$$R_{cc'} = R_{cc'}^0 + \sum_{\lambda=1}^{\Lambda} \frac{\gamma_{\lambda c} \gamma_{\lambda c'}}{E_{\lambda} - E - i\Gamma_{\lambda\gamma}/2}, \quad (51)$$

and to replace the sums in $R_{cc'}^0$ by integrals,

$$\begin{aligned} R_{cc'}^0 &= \left(\sum_{\lambda=-\nu}^{\infty} - \sum_{\lambda=1}^{\Lambda} \right) \frac{\gamma_{\lambda c} \gamma_{\lambda c'}}{E_{\lambda} - E - i\Gamma_{\lambda\gamma}/2} \\ &\approx \left(\int_{-\infty}^{\infty} - \int_{\bar{E}-I/2}^{\bar{E}+I/2} \right) \frac{dE' E' - E + i\bar{\Gamma}_{\gamma}/2}{D_c (E' - E)^2 + \bar{\Gamma}_{\gamma}^2/4} \langle \gamma_c \gamma_{c'} \rangle. \end{aligned} \quad (52)$$

Here \bar{E} and I are midpoint and length of the interval containing the Λ local levels, D_c is the average level spacing and $\bar{\Gamma}_{\gamma}$ the average radiation width. Since $(E' - E)^2 \gg \bar{\Gamma}_{\gamma}^2/4$ for the distant levels we can neglect $\bar{\Gamma}_{\gamma}^2/4$ in the last expression. Moreover we can neglect the off-diagonal elements of $\langle \gamma_c \gamma_{c'} \rangle$ because of the random signs of the γ_c . Finally we can introduce the usual definitions of the pole strength s_c and the distant-level function R_c^{∞} ,

$$s_c \equiv \frac{\langle \gamma_c^2 \rangle}{D_c}, \quad R_c^{\infty} \equiv \oint_{-\infty}^{\infty} dE' \frac{s_c(E')}{E' - E} \quad (53) \quad (54)$$

where \oint denotes Cauchy's principal value. With all this we obtain the final expression

$$\begin{aligned} R_{cc'} &= \sum_{\lambda=1}^{\Lambda} \frac{\gamma_{\lambda c} \gamma_{\lambda c'}}{E_{\lambda} - E - i\Gamma_{\lambda\gamma}/2} \\ &+ \left[R_c^{\infty} + 2s_c \left(\operatorname{artanh} \frac{E - \bar{E}}{I/2} + \frac{i\bar{\Gamma}_{\gamma} I/4}{I^2/4 - (E - \bar{E})^2} \right) \right] \delta_{cc'}. \end{aligned} \quad (55)$$

In many cases R_c^{∞} and s_c vary little between $\bar{E} - I/2$ and $\bar{E} + I/2$ so that one can treat them as adjustable constants which can be

determined simultaneously with the E_λ and $\gamma_{\lambda c}$ in a shape fit to resonance data in this interval. On the other hand they can be obtained from an optical-model calculation. Thus resonance fits can provide a check on differing optical-model calculations. For a large number of structural-material isotopes effective radii, $R'_c = (1-R_c^\infty)a_c$, were obtained from fits to transmission data. Fig. 5 shows one of the fits. The effective radii thus obtained are consistent with a coupled-channel calculation but not with a spherical optical model as shown in Fig. 6.

Johnson and Winters [18] went even further. They actually determined optical-model potentials for s- and p-wave neutrons interacting with ^{32}S from detailed shape analysis of transmission data. Subtracting the local resonance terms from R_{cc} they obtained the distant-level R-functions shown in Fig. 7. The artanh behavior (cf. Eq. (55)) is clearly seen.

This level-statistical description of the distant-level part of the R-matrix is more convenient than the use of dummy levels outside the range $\bar{E}-I/2 \dots \bar{E}+I/2$ or of expansions of the type $R^0 = A(E-\bar{E}) + B(E-\bar{E})^2 + \dots$. It utilizes only two parameters with a clear meaning, R_c^∞ and s_c , both of which can be obtained from an optical model and then refined in a shape fit. Furthermore, the potential-scattering parameters R_c^∞ and s_c are quite insensitive to extensions of the range of parametrization (inclusion of more resonances), in contrast to dummy levels. Nevertheless, since the purely statistical treatment of distant levels may be inadequate if untypically weak or strong levels are located just outside the interval $\bar{E}-I/2 \dots \bar{E}+I/2$, it is good practice to include such "nearby" levels explicitly in the sum in Eq. (55) whenever possible.

7. DISCRETE BOUND LEVELS

An example of the nearby levels just mentioned are levels just below the elastic threshold ($E_\lambda < 0$). In most cases one bound level per spin state is enough for a good description of low-energy, e.g. thermal, cross sections, provided the level-statistical term of Eq. (55) is employed for all more distant bound (and distant unbound) levels. At sufficiently low energies cross sections with $\ell \geq 1$ are negligible. For $\ell = 0$ one has

$$U_{cc} = e^{-2ik_c a_c} \frac{1+ik_c a_c R_{cc}}{1-ik_c a_c R_{cc}} \quad (c \neq \gamma), \quad (56)$$

with R_{cc} given by Eq. (55), if only elastic scattering and radiative capture are energetically possible. Assuming that one bound level suffices one can solve Eq. (56) for the corresponding sum term in R_{cc} . With $k_c a_c \gamma_{\lambda c}^2 = \Gamma_{\lambda n}/2$, $a_c R_c^\infty = a - R'_c$ and $2k_c a_c s_c = S_0 \sqrt{E/1\text{eV}}$ one gets for Λ discrete unbound levels and 1 bound level with parameters E_0 , Γ_n , Γ_γ

$$\begin{aligned}
 \frac{i\Gamma_n/2}{E_0 - E - i\Gamma_\gamma/2} = & - \sum_{\lambda} \frac{i\Gamma_{\lambda n}/2}{E_{\lambda} - E - i\Gamma_{\lambda\gamma}/2} \\
 & - i \left[k_c (a - R'_0) + S_0 \sqrt{\frac{E}{1 \text{ eV}}} \left(\operatorname{artanh} \frac{E - \bar{E}}{I/2} + \frac{i\bar{\Gamma}_\gamma/I}{1 - \left(\frac{E - \bar{E}}{I/2}\right)^2} \right) \right] \\
 & + \frac{U_{cc} e^{2ik_c a_{c-1}}}{U_{cc} e^{2ik_c a_{c+1}}} \quad (\equiv \Delta_{cc}) . \quad (57)
 \end{aligned}$$

Assuming all E_λ , $\Gamma_{\lambda n}$, $\Gamma_{\lambda\gamma}$ as well as R'_0 , S_0 and $\bar{\Gamma}_\gamma$ to be known and calculating U_{cc} from the cross sections σ_c and $\sigma_{cc} = \sigma_c - \sigma_{c\gamma}$ at some low energy E (e.g. 0.0253 eV), via

$$\operatorname{Re} U_{cc} = 1 - \frac{\sigma_c}{2\pi\lambda_c^2 g_c} , \quad (58)$$

$$\operatorname{Im} U_{cc} = \pm \sqrt{\frac{\sigma_{cc}}{\pi\lambda_c^2 g_c} - \left(\frac{\sigma_c}{2\pi\lambda_c^2 g_c}\right)^2} \quad (59)$$

(cf. Eqs. (1) and (2)) one can evaluate the right-hand side of Eq. (57). Equating the result, Δ_{cc} say, to the left-hand side and separating real and imaginary parts one finds eventually

$$-E_0 = -E + \frac{\operatorname{Im} \Delta_{cc}}{\operatorname{Re} \Delta_{cc}} \frac{\Gamma_\gamma}{2} , \quad (60)$$

$$\frac{\Gamma_n}{2} = - \frac{|\Delta_{cc}|^2}{\operatorname{Re} \Delta_{cc}} \frac{\Gamma_\gamma}{2} . \quad (61)$$

With only two equations for the three unknowns E_0 , Γ_n , Γ_γ we can choose one of them arbitrarily and then calculate the others. The approximate constancy of the radiation widths from level to level suggests to take Γ_γ as the mean radiation width $\bar{\Gamma}_\gamma$ obtained from the Λ discrete unbound levels. The sign ambiguity in Eq. (59) is due to the fact that the cross sections depend on $\operatorname{Re} U_{cc}$ and $|U_{cc}|^2$. Usually the positive sign can be discarded immediately because it yields $E_0 > 0$ contrary to the assumption of a bound level. Note that in Eqs. (57) and (61) all neutron widths are to be calculated at the energy E by

$$\Gamma_{\lambda n}(E) = \Gamma_{\lambda n}(|E_\lambda|) \sqrt{E/|E_\lambda|} = \Gamma_{\lambda n}^0 \sqrt{E} \quad (62)$$

(including that for the bound level, $\lambda = 0$).

Eqs. (60) and (61) are a good approximation also for thermally fissile nuclei for which one finds an additional approximate equation for the fission width of the bound level,

$$\frac{\Gamma_f}{2} = - \frac{|\Delta_{cf}|^2}{\text{Re } \Delta_{cc}} \frac{\Gamma_\gamma}{2} \quad (63)$$

$$\text{with } |\Delta_{cf}|^2 \equiv \frac{\sigma_{cf}}{\pi \lambda_c^2 g_c} - \sum_{\lambda=1}^{\Lambda} \frac{\Gamma_{\lambda n} \Gamma_{\lambda f} / 4}{(E_\lambda - E)^2 + \Gamma_\lambda^2 / 4} - S_o \sqrt{\frac{E}{1 \text{eV}}} \frac{\bar{\Gamma}_f / I}{1 - \frac{(E-E)}{I/2}}, \quad (64)$$

and σ_{cf} being the fission cross section for entrance channel c at energy E .

If, for target nuclei with nonzero spin, the level spins are unknown, and only $g\Gamma_n$ is known for unbound levels instead of g and Γ_n separately, one obtains the prescription

$$-E_o = -E + \frac{\text{Im } \Delta_{nn}}{\text{Re } \Delta_{nn}} \frac{\Gamma_\gamma}{2}, \quad (65)$$

$$\frac{g\Gamma_n}{2} = - \frac{|\Delta_{nn}|^2}{\text{Re } \Delta_{nn}} \frac{\Gamma_\gamma}{2}, \quad (66)$$

$$\frac{g\Gamma_f}{2} = - \frac{|\Delta_{nf}|^2}{\text{Re } \Delta_{nn}} \frac{\Gamma_\gamma}{2}, \quad (67)$$

with

$$\Delta_{nn} = \frac{W_{nn} - 1}{W_{nn} + 1} - \sum_{\lambda=1}^{\Lambda} \frac{ig_\lambda \Gamma_{\lambda n} / 2}{E_\lambda - E - i\Gamma_\lambda / 2} - ik(a - R') - iS_o \sqrt{\frac{E}{1 \text{eV}}} \text{artanh} \frac{E - \bar{E}}{I/2} + S_o \sqrt{\frac{E}{1 \text{eV}}} \frac{\bar{\Gamma}_\gamma / I}{1 - \frac{E - \bar{E}}{I/2}}, \quad (68)$$

$$\Delta_{nf} = \frac{\sigma_f}{\pi \lambda^2} - \sum_{\lambda=1}^{\Lambda} \frac{g_\lambda \Gamma_{\lambda n} \Gamma_{\lambda f} / 4}{(E_\lambda - E)^2 + \Gamma_\lambda^2 / 4} - S_o \sqrt{\frac{E}{1 \text{eV}}} \frac{\bar{\Gamma}_f / I}{1 - \frac{E - \bar{E}}{I/2}}, \quad (69)$$

and

$$W_{nn} = e^{2ika} \left[1 - \frac{\sigma}{2\pi \lambda^2} - i \sqrt{(2ka_{\text{coh}})^2 - \left(\frac{\sigma}{2\pi \lambda^2}\right)^2} \right]. \quad (70)$$

The directly observable total and fission cross sections at energy E are weighted sums over the two s-wave spins, $\sigma = \sum_c g_c \sigma_c$, $\sigma_f = \sum_c g_c \sigma_{cf}$. The total widths are to be approximated by $\Gamma_\lambda \approx \Gamma_{\lambda f} + \Gamma_{\lambda \gamma} + 2g_\lambda \Gamma_{\lambda n}$. The same effective radii R' and strength functions S_0 were assumed for both spin states, as in Eq. (57), and the channel subscript c was dropped for κ_c and k_c . Furthermore we used the relationship between the coherent scattering length a_{coh} and the elastic cross sections for each spin state, $a_{coh} = \sum_c \sqrt{g_c \sigma_{cc}} / 4\pi$. Specialization to one spin state ($I = 0$ or $g_\lambda = g_c$) or to nonfissile nuclei ($\sigma_f = 0$, $\Gamma_{\lambda f} = \Gamma_f = 0$) leads to the prescriptions given above.

It is found that the bound-level parameters found with this prescription are usually quite adequate to reproduce all measured partial cross sections not only at the chosen (e.g. thermal) energy but over the whole low-energy range. The lower limit of the range of explicitly given resonances can be taken e.g. as two mean level spacings below the lowest unbound level, $\bar{E} - I/2 = E_1 - 2D$, or one level spacing below the neutron threshold, $\bar{E} - I/2 = -D$. Sometimes it is necessary to shift it towards lower energies to get consistent results ($\bar{E} - I/2 < E_0 < 0$) but in general the calculated cross sections are not sensitive to the exact choice. Figs. 8 and 9 show low-energy cross sections obtained with this method for ^{241}Am with one bound level. The fit to the measured data is quite comparable to that in [18] where no less than 5 bound levels were used.

8. MODERN PROCEDURES IN RESONANCE ANALYSIS

This last section is devoted to the more general problem of non-linear parameter estimation as encountered in resonance analysis of neutron data. As more and better shape analysis codes become operational (see [1] and [2]) area analysis methods are phased out. It is not true that shape analysis fails and must be replaced by area analysis if instrumental resolution is bad, as is often stated. Actually shape analysis is always more convenient because it can deal with many resonances simultaneously, and with a reasonable description of the resolution function its results are not inferior but most of the time superior to area analysis results. It is just the case of only partially resolved multiplets where shape analysis, treating all components simultaneously, gives better results more rapidly than area analysis, where difficult wing corrections must be applied to each component and often several iterations are required to get the final results for the whole multiplet.

So far shape analysis codes employed what may be called primitive least-squares techniques: (1) correlations among data points, due e.g. to common background subtraction or normalization, are neglected, (2) prior knowledge about the cross section parameters is used at best in a very limited way, namely to fix first guesses for the iteration procedure which in general is re-

quired because of the nonlinearity of the mathematical model (R-matrix theory). Parameter estimation was thus based essentially on the data in hand and the resulting parameters had to be combined with the prior knowledge after the fit by some kind of weighted averaging.

A more rigorous and convenient approach consists in (1) using the full uncertainty information including correlated errors and (2) in combining prior information with the new information contained in the data to be fitted by means of Bayes' theorem and then to search for the most probable parameters. Consider

- observables y_i , $i = 1, 2, \dots, I$ (e.g. transmissions)
- parameters x_μ , $\mu = 1, 2, \dots, M$ (cross section parameters)
- a model $y = y(x)$ (R-matrix theory)

where $y = (y_1, y_2, \dots, y_I)$, $x = (x_1, x_2, \dots, x_M)$ are vectors in the data and parameter spaces, respectively, and $I > M$. Suppose

- (a) that even before the data y_i became available one had some prior knowledge about the parameters x_μ , namely estimates ξ_μ and correlated errors $M_{\mu\nu}$ (or at least variances $M_{\mu\mu}$), so that the probability for x to be the true value, given ξ , can be taken as

$$p(x|\xi) \propto \exp\left[-\frac{1}{2}(x-\xi)^+ M^{-1} (x-\xi)\right] \quad (71)$$

where $^+$ denotes the transpose;

- (b) that a new measurement yielded values η_i and correlated errors V_{ik} for the observables y_i , so that the likelihood to obtain these values provided the true parameter vector is x , can be taken as

$$p(\eta|y) \propto \exp\left[-\frac{1}{2}(\eta-y(x))^+ V^{-1} (\eta-y(x))\right] . \quad (72)$$

The assumption of multi-variate Gaussians in (71) and (72) is an approximation which may fail for large distances $|x-\xi|$ and $|\eta-y(x)|$ but for small distances it is expected to be reasonable and in any case sufficient for parameter estimation purposes.

One can now combine the prior probability (71) and the likelihood (72) by means of Bayes' theorem to get the probability density function for x , given the data η and the prior estimates ξ ,

$$\begin{aligned} p(x|\xi\eta) &\propto p(\eta|x)p(x|\xi) \\ &\propto \exp\left[-\frac{1}{2}(x-\xi)^+ M^{-1} (x-\xi) - \frac{1}{2}(\eta-y(x))^+ V^{-1} (\eta-y(x))\right] . \quad (73) \end{aligned}$$

The most probable vector x is the one that minimizes the exponent,

$$(x-\xi)^+ M^{-1} (x-\xi) + (n-y(x))^+ V^{-1} (n-y(x)) \equiv \chi^2 = \min . \quad (74)$$

We shall consider this particular parameter vector as the improved estimate and call it ξ' . Note that without prior knowledge M^{-1} , and thus the first term, vanishes. Neglecting then also the off-diagonal elements of V^{-1} one gets the starting condition for primitive least-squares fitting as used in conventional shape analysis of nuclear resonance data.

The condition (74) is equivalent to

$$M^{-1} (x-\xi) - \dot{y}(x)^+ V^{-1} (n-y(x)) = 0 \quad (75)$$

where \dot{y} is the rectangular matrix of sensitivity coefficients,

$$\dot{y}_{i\mu} = \frac{\partial y_i}{\partial x_\mu} . \quad (76)$$

Eq. (75) is easily solved for x if y is a linear function of x . In nuclear resonance work, however, $y(x)$ is nonlinear and one must iterate, for instance with the Newton-Raphson method (in M dimensions). Starting with the prior most probable values, $x_0 = \xi$, one finds after n steps

$$x_{n+1} = \xi + [M^{-1} + \dot{y}(x_n)^+ V^{-1} \dot{y}(x_n)]^{-1} \dot{y}(x_n)^+ V^{-1} [n-y(x_n) - \dot{y}(x_n)(\xi-x_n)]$$

and finally the new estimate

$$\xi' = \xi + [M^{-1} + \dot{y}(x_\infty)^+ V^{-1} \dot{y}(x_\infty)]^{-1} \dot{y}(x_\infty)^+ V^{-1} [n-y(x_\infty) - \dot{y}(x_\infty)(\xi-x_\infty)] . \quad (77)$$

The new correlated errors are obtained as follows. We consider a small domain around $x = x_\infty = \xi'$ where $y(x)$ can be considered to be linear. Then the right-hand side of (73) reduces to a product of two multivariate Gaussians which is equivalent to another multivariate Gaussian with the most probable value $x = \xi'$ and correlated errors given by

$$M'^{-1} = M^{-1} + \dot{y}(x_\infty)^+ V^{-1} \dot{y}(x_\infty) . \quad (78)$$

In practice, of course, one does not need infinitely many iterative steps as the notation x_∞ implies. Usually half a dozen steps or less are quite enough.

Sometimes it is better to write everything in terms of the covariance matrices M and V instead of their inverses. For instance, a common (systematic) background uncertainty in the data, $\delta\eta_i = b$, leads to $V_{ik} = \delta\eta_i\delta\eta_k = b^2$. The matrix V is then singular and V^{-1} is undefined. It can be shown that Eqs. (77) and (78) are equivalent to

$$\xi' = \xi + \dot{M}y(x_{\infty})^+ [V + \dot{y}(x_{\infty})\dot{M}y(x_{\infty})^+]^{-1} [\eta - y(x_{\infty}) - \dot{y}(x_{\infty})(\xi - x_{\infty})] , \quad (79)$$

$$M' = M - \dot{M}y(x_{\infty})^+ [V + \dot{y}(x_{\infty})\dot{M}y(x_{\infty})^+]^{-1} \dot{y}(x_{\infty})M . \quad (80)$$

The pairs of equations (77), (78) and (79), (80) show explicitly how the prior estimates and uncertainties ξ , M are updated by new data η, V so that the new (posterior) estimates and uncertainties are ξ', M' . The minus sign in Eq. (80) corresponds to the reduction of the uncertainties by the new data. The change of the estimates and the reduction of the uncertainties is seen to be small if the sensitivity coefficients $\dot{y}_{i\mu}$ are small and vice versa.

This iterative least-squares approach with full account of parameter and data correlations and of prior information is implemented in the shape analysis code SAMMY that is being developed at ORNL by F. Perey and Nancy Larson. So far the code, which uses the Reich-Moore formalism, works for transmission data. An extension to capture data is under development. Even in its present state the code has clearly shown the advantage of including the prior probability (71). This allows mathematically straightforward incorporation of prior knowledge in the fit procedure and at the same time constrains the parameter search to a reasonable domain in a smooth way, avoiding the problems of sharp limits typical for linear programming. Moreover, uncorrelated portions of the data can be analyzed successively in separate runs, proper transfer of the accumulated information from one run to the next being ensured.

9. CONCLUSIONS

A short characterization of the practically available multi-level formalisms was given. The fact that the Reich-Moore formalism can be considered as automatically ensuring unitarity of the collision matrix makes it universally applicable to light and heavy nuclei, with weakly or strongly overlapping levels, near thresholds, transmission windows and resonance peaks. Actually most modern shape fitting codes use variants of the Reich-Moore formalism. The Adler-Adler representation does not automatically guarantee unitarity unless obtained by conversion from Reich-Moore parameters. As it neglects the energy dependence of total widths it leads to errors for light and medium-weight nuclei, especially

near thresholds. The MLBW approximation is definitely non-unitary and in case of strong level overlap, near cross section peaks and minima often necessitates large corrections. In the ENDF file these are given as a "smooth" cross section component which, however, is often not smooth at all.

Doppler broadening can be calculated by means of the Voigt profiles. This is very fast with Adler-Adler parameters (time proportional to number of resonances), slow with MLBW and Reich-Moore parameters (time proportional to squared number of resonances, with additional time needed for conversion to Kapur-Peierls form at each energy in case of Reich-Moore parameters). A new prescription, however, yields Doppler-broadened Reich-Moore and MLBW cross sections about equally fast as Adler-Adler cross sections. The trick is to apply Turing's method for Gaussian broadening to the multi-level cross section expressions directly rather than to the zero-temperature Voigt profiles. The necessity to convert Reich-Moore parameters to Kapur-Peierls parameters is then reduced to the resonance energies of narrow levels instead of all energies. In view of these developments it appears appropriate to reconsider the question whether Reich-Moore parameters should not be readmitted to the ENDF/B file.

Further recent developments in resonance cross section work concern the representation of distant levels. It is found that a level-statistical treatment of the distant-level part of the R-matrix, involving strength functions and effective radii either as fit parameters or as quantities obtained from optical-model calculations, is the most rigorous and convenient way to deal with edge effects in resonance fits. This approach can also be used to determine the parameters of representative bound levels from those of discrete unbound and distant bound and unbound levels and from the thermal cross sections.

Finally attention was drawn to the possibility to improve existing shape analysis codes by allowing for correlated data errors and by formalized inclusion of prior information by means of Bayes' theorem.

REFERENCES

1. F. H. FRÖHNER, "Applied Neutron Resonance Theory," in Nuclear Theory for Applications, IAEA, Vienna, 1980; also available as report KfK 2669 (1978).
2. G. M. HALE, "Use of R-matrix Methods for Light Element Evaluations," Workshop on Evaluation Methods and Procedures, these proceedings.
3. E. P. WIGNER and L. EISENBUD, Phys. Rev. 72 (1947) 29,
E. P. WIGNER, J. Am. Phys. Soc. 17 (1949) 99.

4. A. M. LANE and R. G. THOMAS, Rev. Mod. Phys. 30 (1958) 257.
5. P. L. KAPUR and R. E. PEIERLS, Proc. Roy. Soc. (London) A166 (1938) 277; R. E. PEIERLS, Proc. Cambridge Phil. Soc. 44 (1947) 242.
6. C. W. REICH and M. S. MOORE, Phys. Rev. 111 (1958) 929.
7. D. R. HARRIS, Neutron Cross Sections and Technology, Washington D.C., 1966 (CONF 660303), p. 833.
8. B. J. ALLEN, A. R. DE L. MUSGROVE and W. K. BERTRAM, Neutron Data of Structural Materials for Fast Reactors, Oxford etc., 1979, p. 497.
9. M. K. DRAKE (ed.), "Data Formats and Procedures for the ENDF Neutron Cross Section Library," report ENDF 102, (1970).
10. F. T. ADLER and D. B. ADLER, Nucl. Data for Reactors, IAEA, Vienna, 1970.
11. G. DE SAUSSURE and R. B. PEREZ, report ORNL-TM-2599 (1969).
12. F. H. FRÖHNER, Neutron Physics and Nuclear Data, Harwell, 1978, p. 306.
13. G. A. KORN and T. M. KORN, Mathematical Handbook for Scientists and Engineers, New York etc., 1961, p. 367.
14. M. R. BHAT and G. E. LEE-WHITING, Nucl. Instr. Meth. 47 (1967) 277.
15. A. M. TURING, Proc. London Math. Soc., Ser. 2, 48 (1943) 180.
16. A. W. SOLBRIG, JR., Nucl. Sci. Eng. 10 (1961) 167, see also Ref. [1] p. 69.
17. B. E. WATT, Phys. Rev. 87 (1952) 1037, see also D. G. MADLAND, "Prompt Fission Neutron Spectra and v_p ," these proceedings.
18. J. E. LYNN, B. H. PATRICK, M. G. SOWERBY and E. M. BOWEY, Report AERE-R 8528 (1979).
19. C.H. Johnson and R.R. Winters, Phys. Rev. C21(1980)2190
20. SWEDISH NUCLEAR DATA COMMITTEE, "Compilation of Actinide Neutron Nuclear Data", Report KDK-35 (1979)
21. H. Beer and R.R. Spencer, "keV Neutron Radiative Capture and Total Cross Sections", Report KfK 2063(1974)

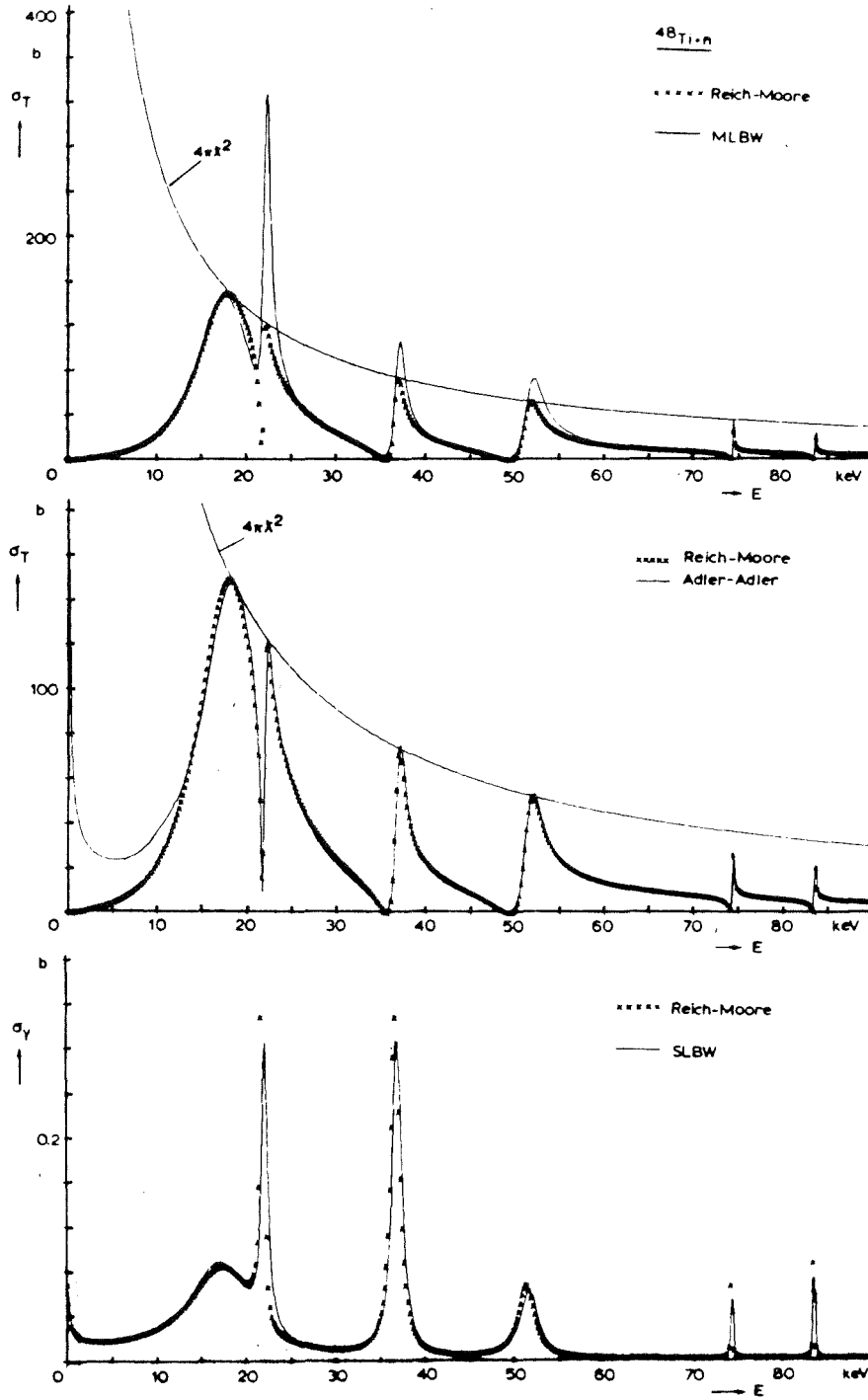


Fig. 1 a-c Illustration of inadequacy of approximations admitted by ENDF/B conventions for medium-mass nuclei. Reich-Moore values are exact. The unitarity limit $\sigma_T < 4\pi\lambda^2$ is seriously violated by MLBW, less by Adler-Adler. The latter fails at low energies [12].

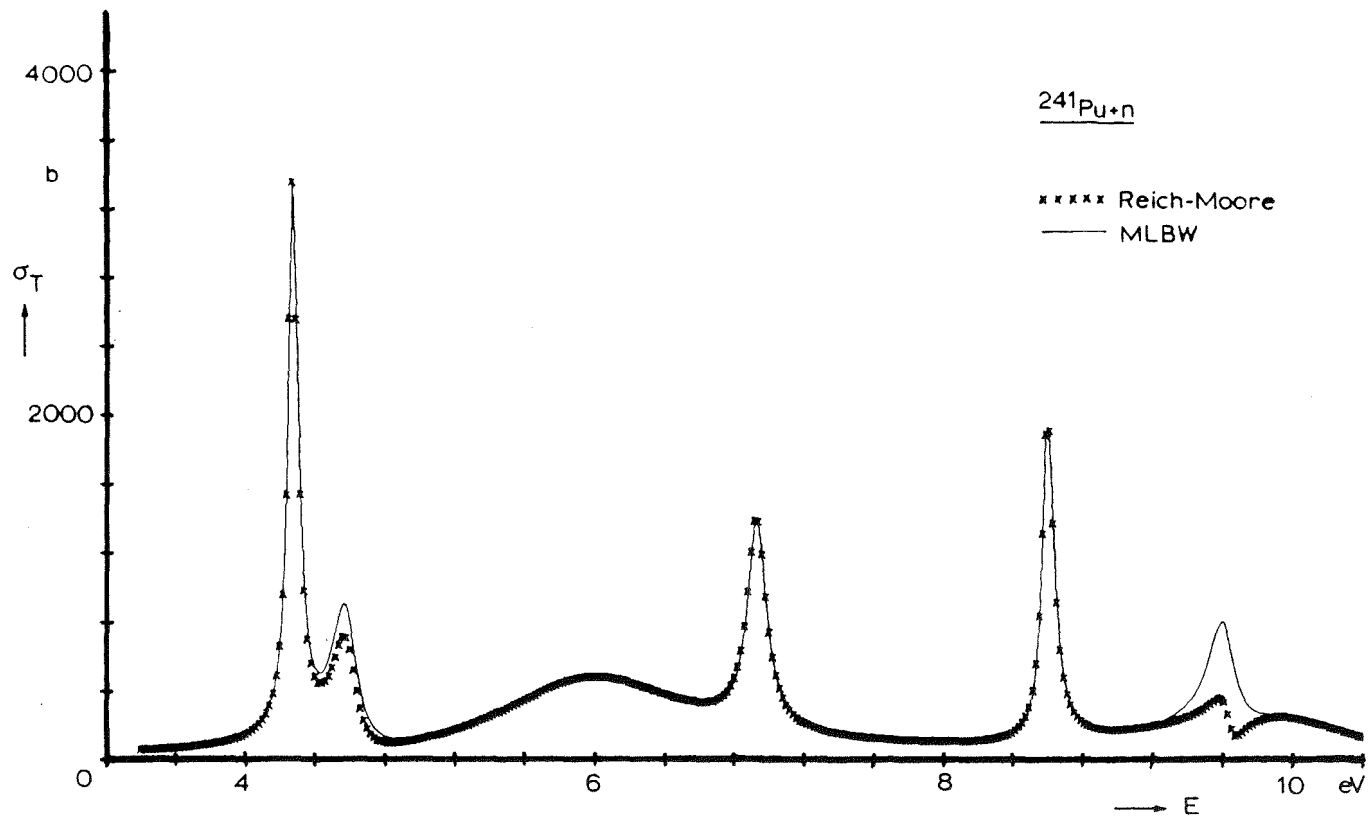


Fig. 1 d Example for failure of MLBW approximation to reproduce strongly interfering doublets in the total cross section of a heavy nuclide. Reich-Moore values are exact, calculated with two open fission channels.

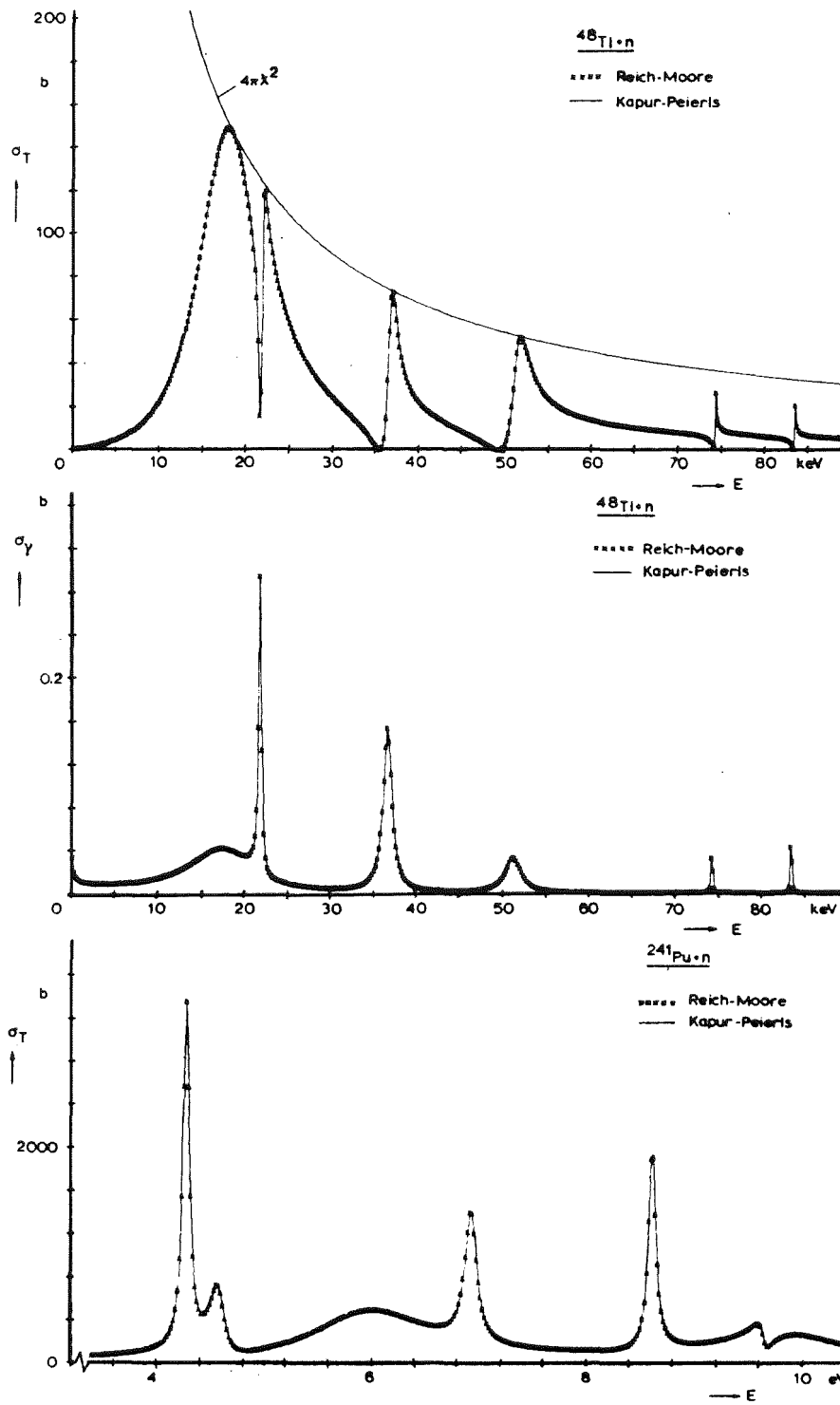


Fig. 2 Verification of Reich-Moore/Kapur-Peierls conversion prescription, Eqs. 41 and 37, for a light and a heavy, fissile nuclide. Reich-Moore values were calculated directly from unconverted, Kapur-Peierls curves from converted resonance parameters [12].

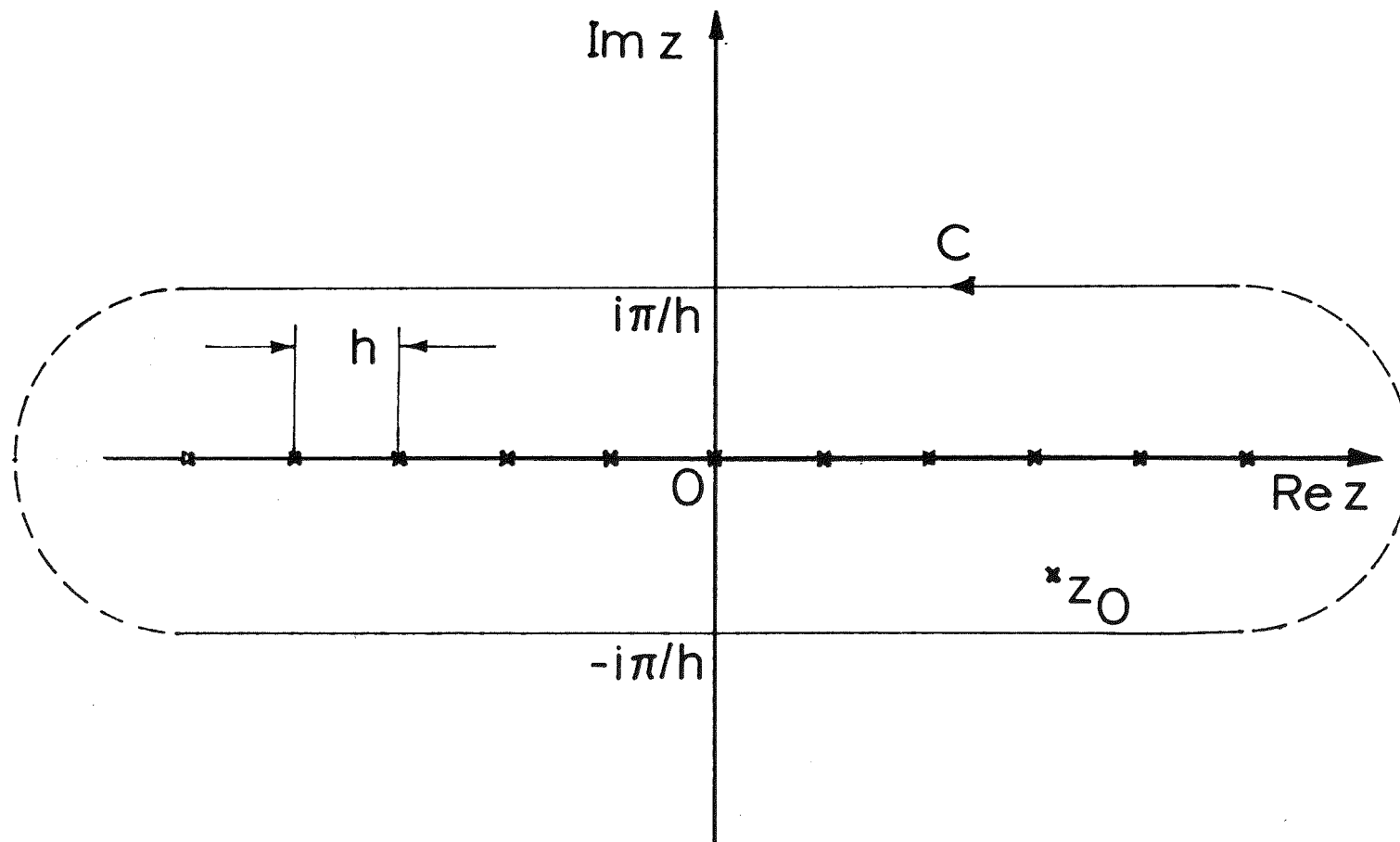


Fig. 3 The contour (C) and the poles (x) for Turing's integral, Eq. 44.

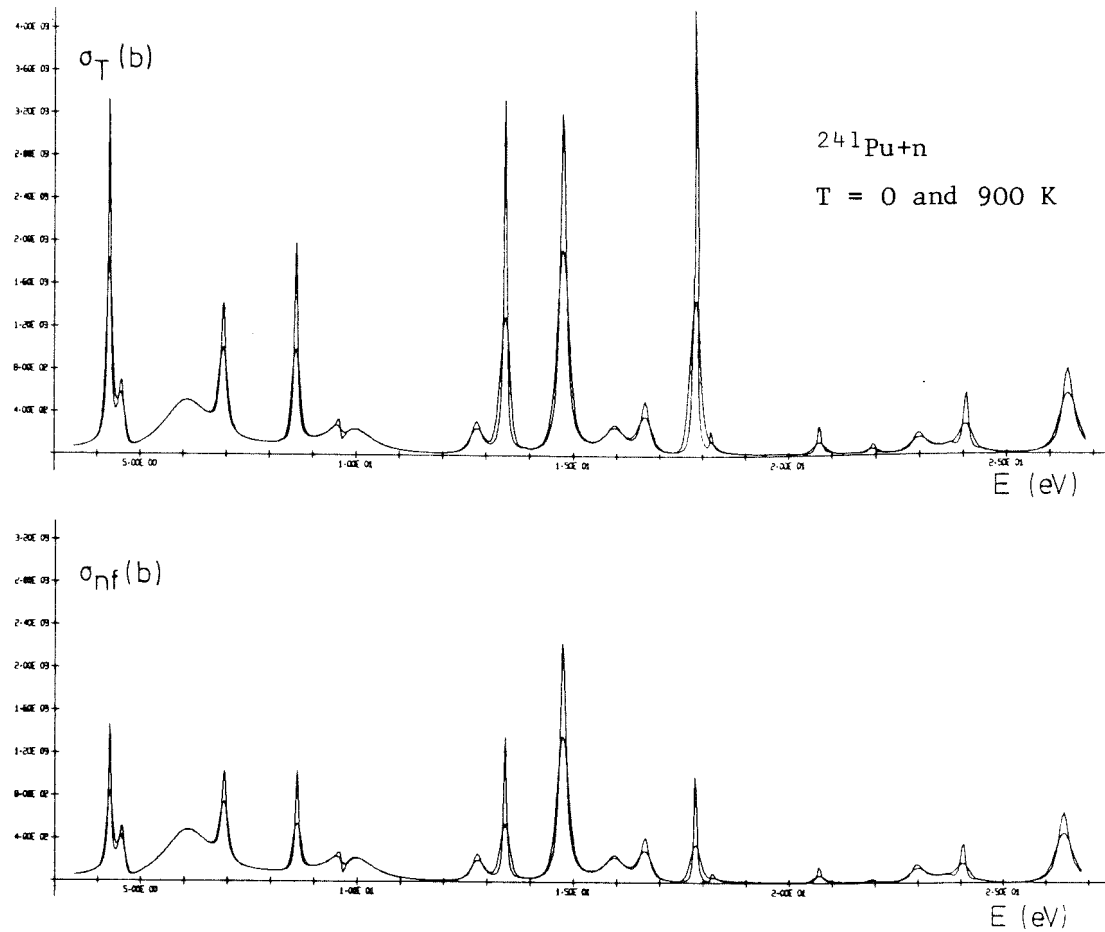


Fig. 4 a-b

Natural and Doppler-broadened total and fission cross sections of $^{241}\text{Pu}+n$, calculated with a 3-channel Reich-Moore formalism and direct application of Turing's method to the multi-level cross section expressions (i.e. without Voigt profiles).

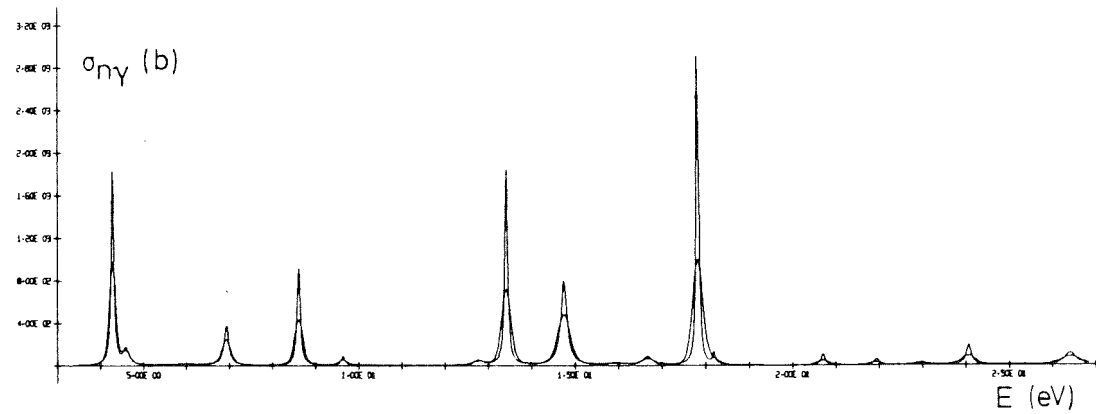
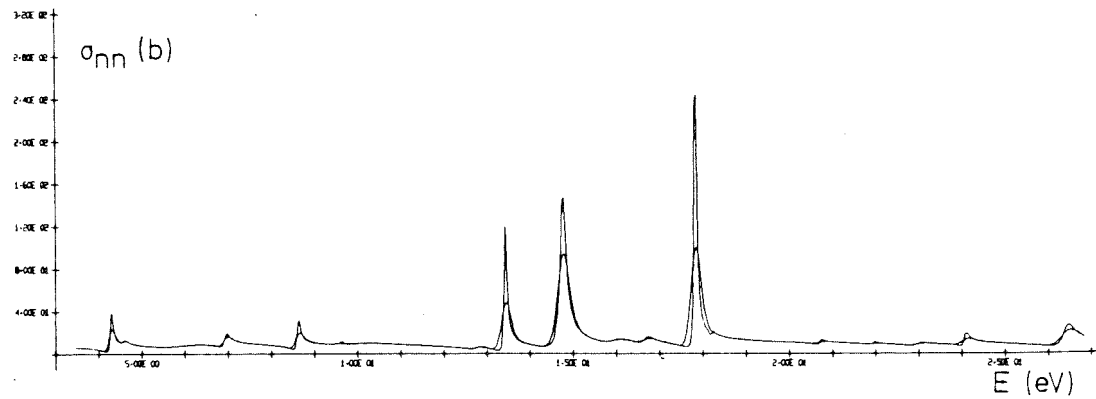


Fig. 4 c-d Natural and Doppler-broadened scattering and capture cross sections of $^{241}\text{Pu}+n$, calculated with 3-channel Reich-Moore formulae and direct application of Turing's method (i.e. without Voigt profiles). The complete set of cross sections between 4.5 and 27 eV shown in Figs. 4 a-d, involving 35 resonances and 760 energies, was generated within 3.7 s on an IBM/370-168 computer.

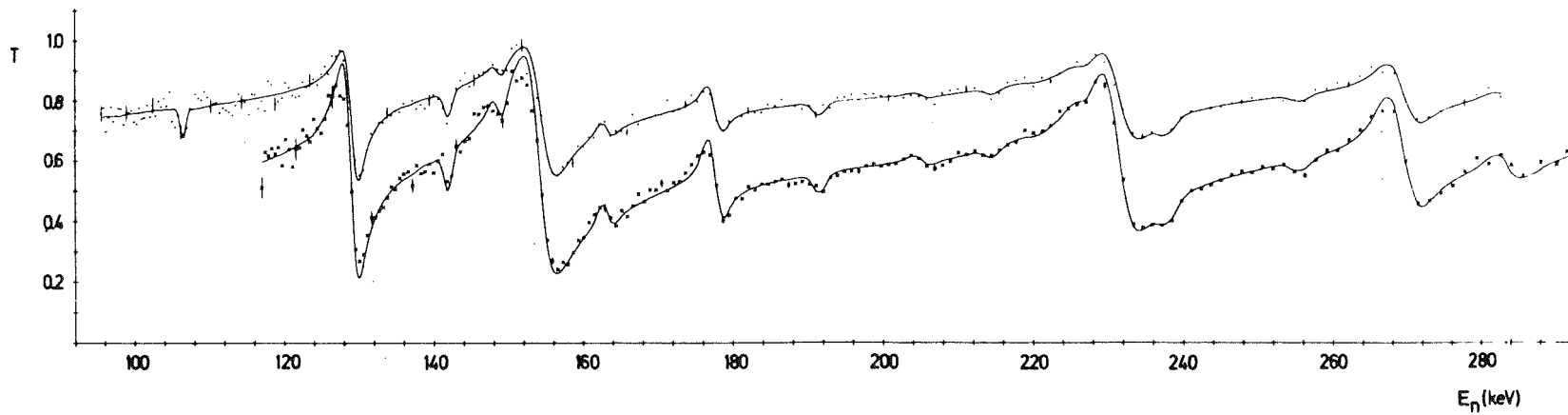


Fig. 5 Shape fits to two sets of transmission data simultaneously with the level-statistical treatment of distant levels, Eq. 55. Note the consistently good fit even near the limits of the range of the fit (from [21]).

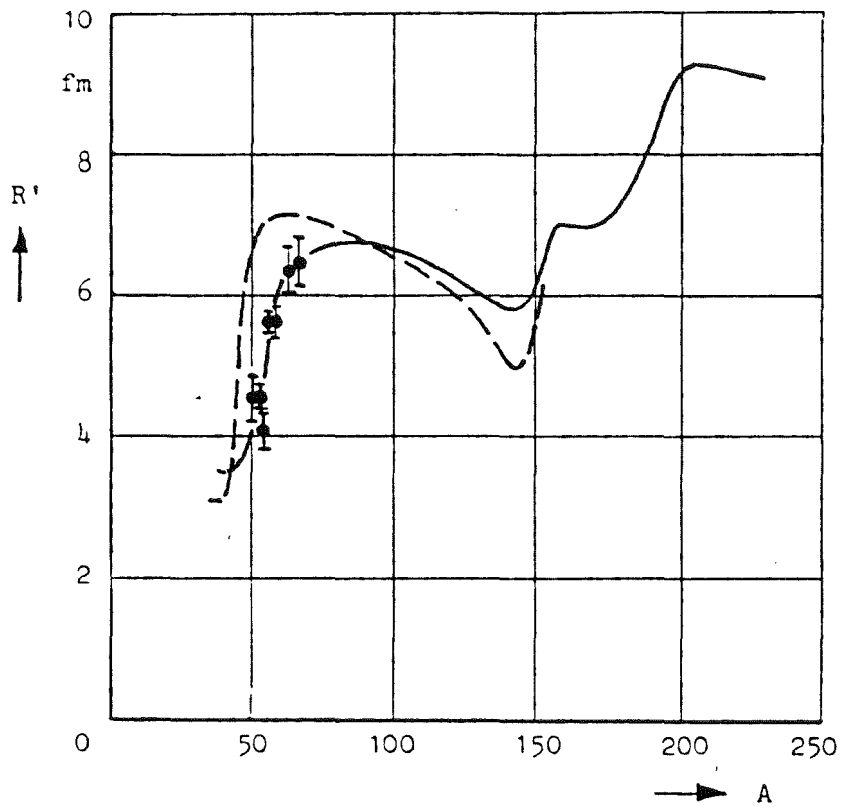


Fig. 6 Effective nuclear radii obtained for Cr, Fe and Ni isotopes by shape fits to transmission data below 300 keV with the level-statistical treatment of distant levels, Eq. 55. The broken curve was calculated with a spherical, the solid line with a deformed optical potential (see [1] for further references).

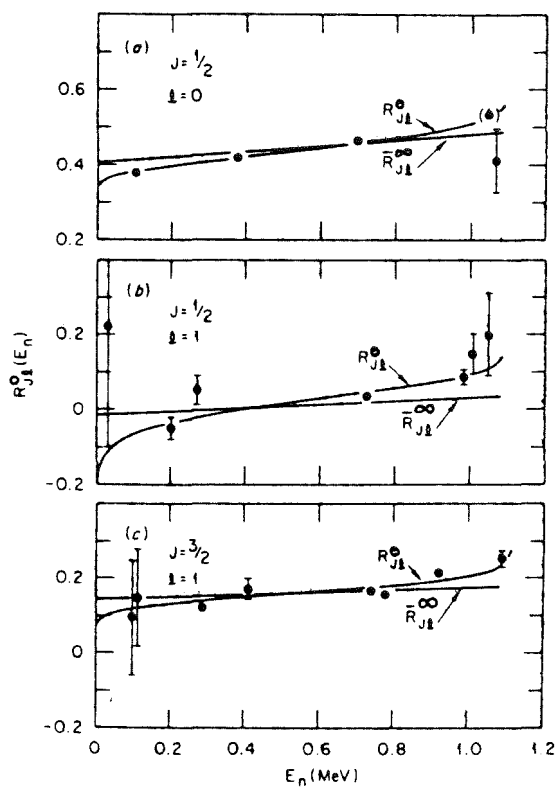


Fig. 7 Distant-level R-functions obtained by Johnson and Winters from transmission shape fits [19]. Solid circles: total R-function minus local-level sum, curve: optical-model calculation. The ar tanh behavior (cf. Eq. 55) is clearly seen. R^∞ is taken not as a constant as in Eq. 55 but as a linear function of energy.

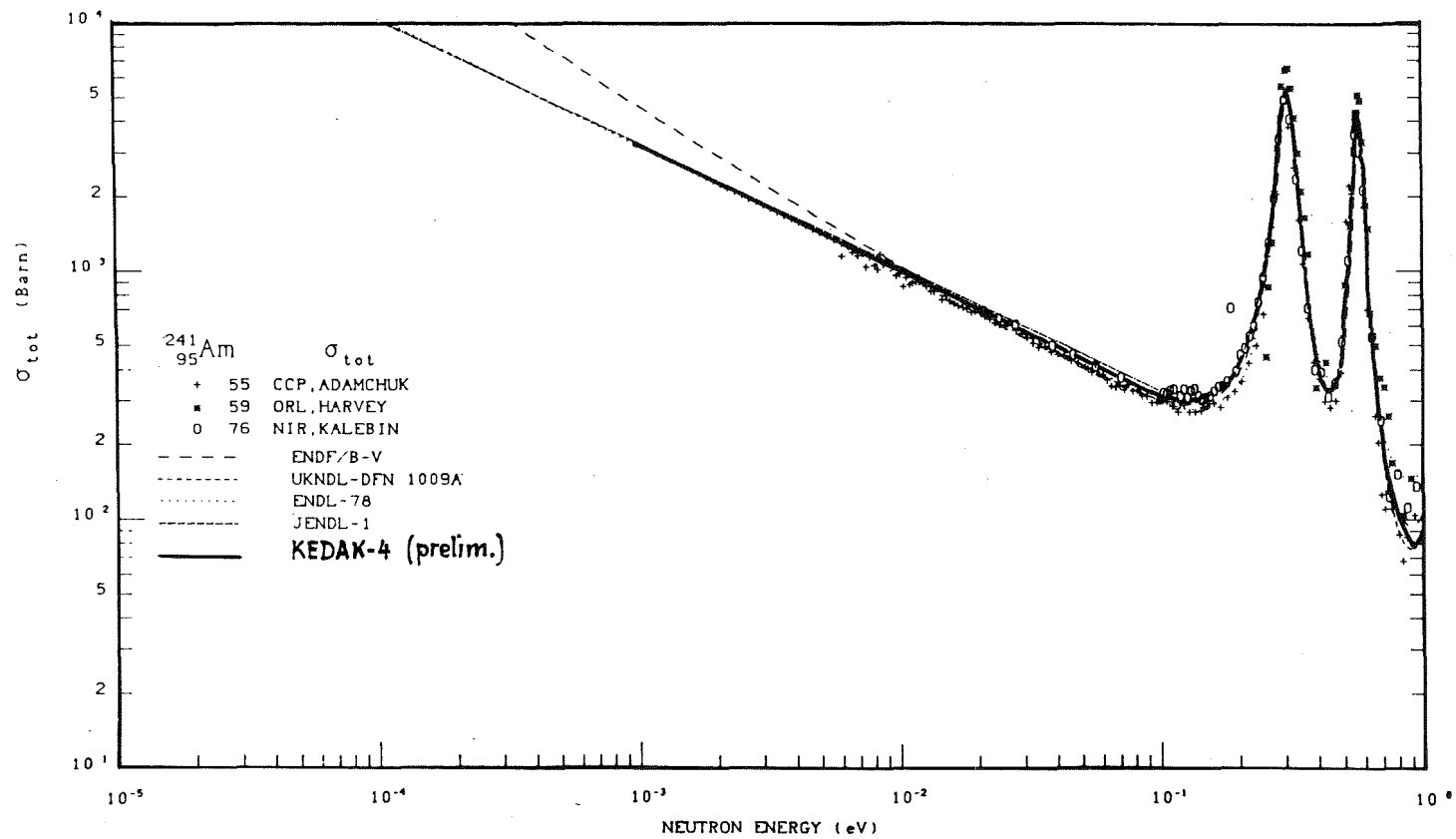


Fig. 8 Comparison between measured and evaluated total cross sections of $^{241}\text{Am}+n$ [20]. The KEDAK-4 curve was calculated with distant-level terms according to Eq. 57 and one bound level adjusted so as to reproduce the 2200 m/s cross sections.

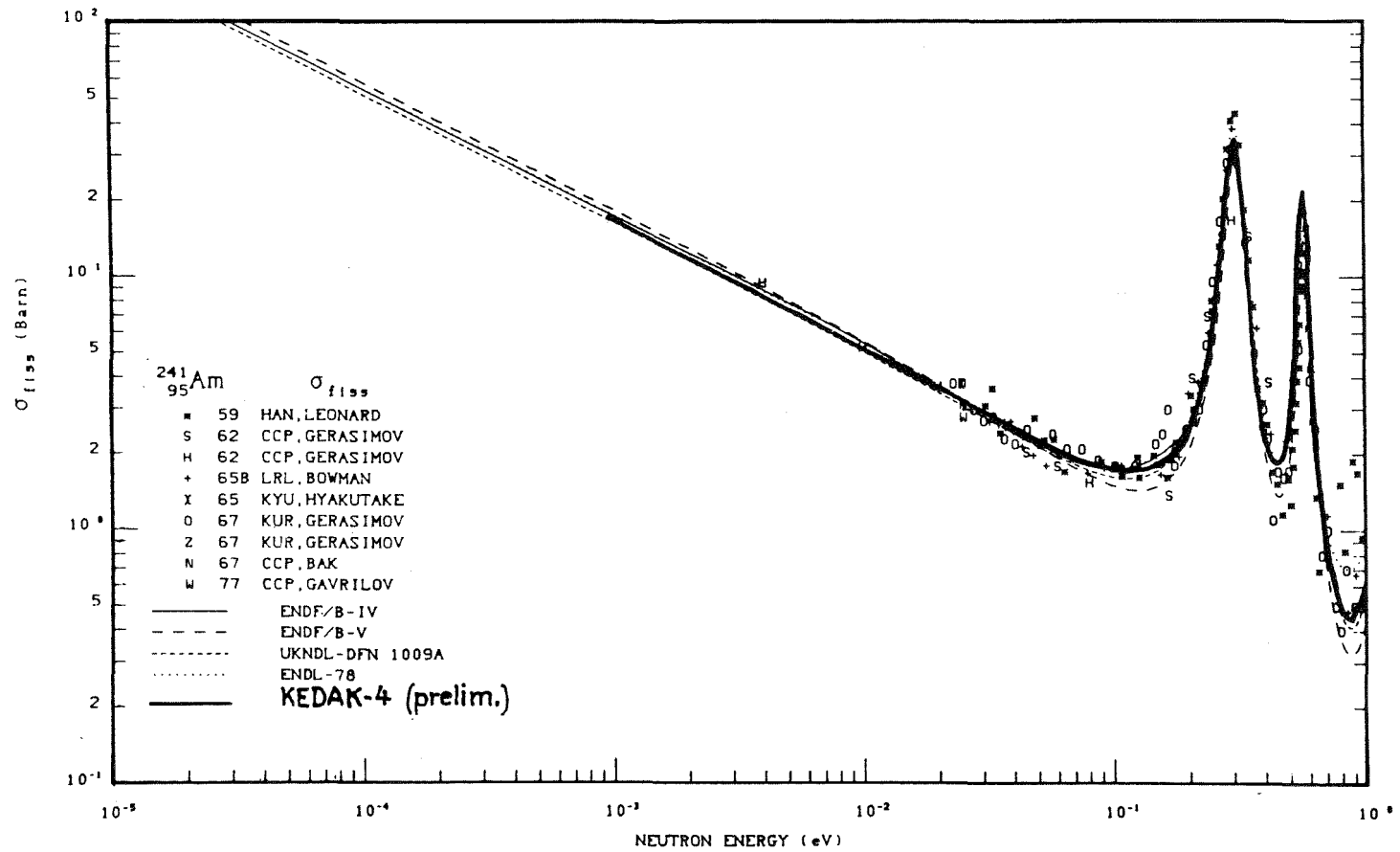


Fig. 9 Comparison between measured and evaluated fission cross sections of $^{241}\text{Am}+n$ [20]. The KEDAK curve was calculated with distant-level-terms according to Eqs. 68-70 and one bound level adjusted so as to reproduce the 2200 m/s cross sections.